ES Mater. Manuf., 2021, **13**, 66-75

ES Materials and Manufacturing

DOI: https://dx.doi.org/10.30919/esmm5f447

A Sustainable Synthesis of Nickel-Nitrogen-Carbon Catalysts for Efficient Electrochemical CO_2 Reduction to CO

John Pellessier, Yang Gang and Ying Li*

Abstract

The electrochemical CO_2 reduction reaction (CO_2RR) is a promising approach of using renewable power sources such as wind and solar to convert CO_2 into value-added products. However, conventional methods of synthesizing high-performance CO_2RR catalysts usually produce wastes and are not environmentally friendly. Herein, we developed a sustainable catalyst synthesis method by using cheap, abundant cornstarch as the feedstock, and doping it with nickel (Ni) from a simulated metal-containing wastewater, before finally doping it with nitrogen (N) to create a highly efficient metal-nitrogen-carbon (M-N-C) catalyst that is dominated by single atomic Ni sites without the need for an acid wash post-treatment. The cornstarch-based catalyst demonstrated a high faradaic efficiency (FE) of 92% for CO production with a CO current density of 11.6 mA/cm^2 at −0.8 V versus reversible hydrogen electrode (RHE). At the same Ni content under the same testing conditions, a catalyst prepared via conventional wet impregnation only attained a CO current density of 9.3 mA/cm^2, and a catalyst prepared using more expensive graphene oxide achieved a CO current density of 11.5 mA/cm^2 but with a lower FE (CO) at 81%. Findings from this work provide insights into using low-cost sustainable biomaterials and non-waste producing methods to produce effective electrochemical CO_2RR catalysts.

Keywords: Electrochemical CO_2 reduction; CO Production; Biomaterials; Heavy Metals; Sustainable Manufacturing.
Received date: 13 March 2021; Accepted date: 30 March 2021.
Article type: Research article.

1. Introduction

Rising waste levels, be them solid, liquid, or gas, are posing greater and greater threats to human life. The US Environmental Protection Agency (EPA) estimated that American homes produced 40.7 million tons of municipal wastes in 2017[1] and output nearly 7,000 million metric tons of greenhouse gases in 2018.[2] Industrial processes such as metal finishing and electroplating also produce wastewater containing toxic heavy metals such as iron (Fe), zinc (Zn), or nickel (Ni), in concentrations of 10 – 1000 ppm before treatment.[3,4] As a result, a considerable amount of research has been conducted on how to reduce the production of wastes and meanwhile reuse the generated solid, liquid, and gas wastes. Some of these techniques include composting leftover biomaterial,[5] adsorption of heavy metals from wastewater onto biopolymers,[4,6] and electrochemical reduction of carbon dioxide (CO_2) into value added products via the CO_2 reduction reaction (CO_2RR).[7]

J. Mike Walker '66 Department of Mechanical Engineering, Texas A&M University, College Station, Texas, 77843, United States.
**E-mail:* yingli@tamu.edu (Y. Li)

While there have been great advances in improving the performance of current CO_2RR catalysts to close the gap required for practical large-scale applications.[7] There have been only a few works that have focused on developing synthesis methods to decrease the cost of the CO_2RR catalysts while keeping the methods sustainable.[8-10] A popular catalyst to study in recent years has been the metal-nitrogen-carbon (M-N-C) based catalyst as it utilizes two of the most abundant elements found on earth, carbon (C) and nitrogen (N), as well as being able to produce good catalytic performance when doped with transition metals like Fe, Ni, or Zn. Currently, a widely accepted method for synthesizing a M-N-C based CO_2RR catalyst is to use wet impregnation to dope a carbon substrate, normally graphene or graphene oxide (GO),[11-13] and carbon nanotubes (CNT),[14] with a metal precursor and a N precursor, which is then pyrolyzed and quite often post treated with an acid wash to remove metal nanoparticles that favor hydrogen evolution reaction,[15-21] leaving only M-N-C active sites for high CO production selectivity.[17, 22] While producing catalysts with good performance this materials synthesis method is not sustainable and not easy to scale up because of the complex synthesis process and the waste-producing pre- or post-treatment steps.

First, commonly used carbon substrates such as GO and CNT often require complex steps for synthesis and thus are expensive.[8] There is a strong need to identify a more sustainable carbon source that is abundant and renewable. Cornstarch is a renewable biomass that is already widely produced. Despite the already abundant uses of cornstarch in applications such as food preparation and in the production of packing peanuts, large quantities of cornstarch are wasted and eventually end up in landfills instead of being reused or recycled.[23] This research thus explores the potential of this abundant, easy to acquire biomaterial as the carbon source for CO_2RR catalysts.

Second, the pre- or post-treatment processes such as acid washing the M-N-C catalysts to remove metal nanoparticles. This creates heavy metal containing liquid wastes, which can cause various cancers and neurological issues for humans even at concentrations less than 1 mg/L or 1 ppm,[4,24] and cause adverse effects on aquatic and plant life.[25] Therefore, there is a strong need for an alternative catalyst synthesis method to avoid this waste-producing step, or even more desirable, to use metal-containing wastes already produced from industrial processes to supply the metal needed for the catalysts. Known waste streams with high metal ion concentrations include those from the metal finishing and electroplating industries. While the ability of biopolymers adsorbing heavy metals from wastewater has been demonstrated before,[4,6] to our knowledge there is little research on the reuse of these heavy metal containing biopolymers. Cornstarch as a renewable biopolymer can be used to adsorb positively charged metal ions from solution as it has a structure naturally suited for the adsorption of metal ions due to its large concentration of negatively charged oxygen functional groups as seen in Fig. S1.[11,13]

As mentioned above, typical adsorption of heavy metal ions onto biopolymers creates a by-product of metal containing biomass, which currently have little to no use, while CO_2RR catalyst synthesis often produces metal-containing toxic wastes. To address these issues holistically, we have developed a novel, sustainable synthesis method for efficient CO_2RR catalysts with abundant M-N-C active sites using renewable biopolymers (*e.g.* cornstarch) and metal (*e.g.* Ni) containing solution as the feedstock, without the need of an acid wash post treatment to remove excess metal nanoparticles, thus cutting down on toxic waste production during synthesis. The overall catalyst synthesis and CO_2RR process is illustrated in Fig. 1, which is truly sustainable involving the utilization of three wastes (*i.e.* gaseous CO_2, metal-containing liquid solution, and solid biomass) to generate value-added products such as CO using renewable solar and wind power as the energy source. These sustainably synthesized catalysts have also demonstrated comparable CO_2RR performance to those benchmark catalysts synthesized by widely used methods and leading catalysts reported in literature.

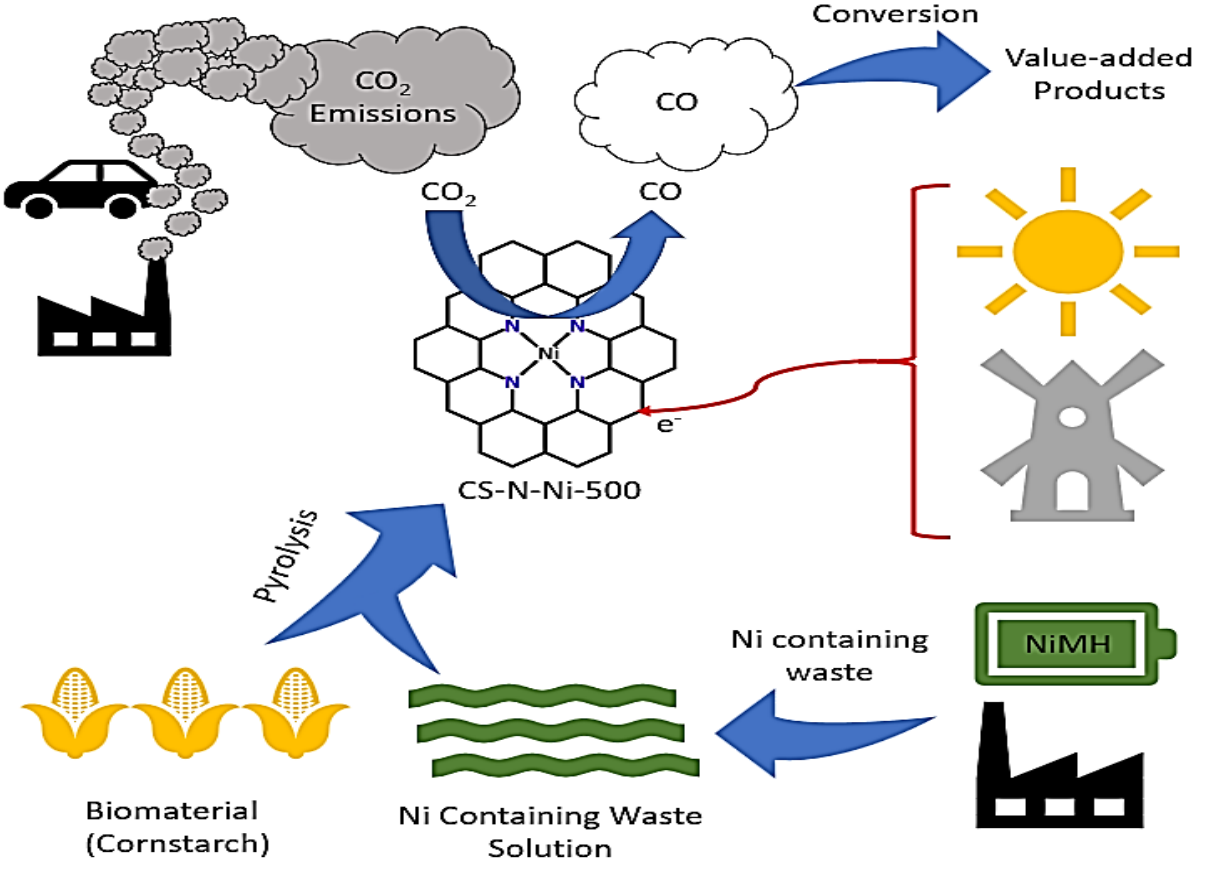

Fig. 1 Graphical illustration of the process for incorporating biomaterials and heavy metal containing waste solutions into the synthesis of CO_2RR catalysts.

2. Experimental

2.1 Synthesis of Catalysts

2.1.1 Synthesis of CS-N-Ni catalysts based on cornstarch

The CS-N-Ni catalysts were synthesized as follows. To begin, 1.0 g of cornstarch (Argo) was mixed into a 50 mL nickel nitrate solution at a Ni^{2+} concentration in the range of 10 – 1000 ppm. This range simulates Ni concentrations that can be found in real world waste sources such as industrial plating effluent[26] and from waste streams generated from disposed nickel-metal hydride batteries.[27] This cornstarch-Ni mixture was vigorously stirred for 24 h, after which it was centrifuged at 13000 RPM for 5 min. Following centrifuging the supernatant was poured off. The remaining pellet was then dried in a 60 °C oven overnight and ground to homogeny. To prepare for pyrolysis 100 mg of ground pellet was further ground to homogeny with 1.0 g of urea to dope with nitrogen during pyrolysis. The pyrolysis process was carried out in a tube furnace under 100 sccm (standard cubic centimeter per minute) argon (Ar) (Airgas, UHP grade). The temperature was heated up to 900 °C with a heating rate of 3 °C/min and held for 1 h at 900 °C, after which the system was cooled down to ambient conditions naturally. The obtained catalyst was denoted CS-N-Ni-X, where X in the range of 10 – 1000 represents the ppm concentration of Ni in the precursor solution.

Besides the CS-N-Ni-X samples, the following control samples were also prepared: CS, where just 100 mg of cornstarch was pyrolyzed (without Ni and N), and CS-N where 100 mg of cornstarch and 1.0 g of urea were ground together and pyrolyzed (without Ni). Both were prepared under the same heating rate, max temperature, and gaseous environment as above. In addition, an acid washed version of CS-N-Ni-500 (CS-N-Ni-500-AW) was prepared where 50 mg of CS-N-Ni-500 was washed with 15 wt% HCl five times and ethanol twice then dried in a vacuum oven over night. This acid wash treatment would remove excess metal nanoparticles on the catalyst, if any, leaving only well dispersed atomic sites.[19]

2.1.2 Synthesis of GO-N-Ni catalysts based on graphene oxide

Since GO is one of the most popular and active supports for M-N-C catalysts reported in the literature, this group of catalysts were synthesized using graphene oxide (GO) and their performance compared with those using cornstarch. The synthesis of GO follows a typical acid and oxidant treatment as published in a previous report.[28] As such, 0.75 g of raw graphene, 4.5 g of $KMnO_4$, 90 mL of concentrated H_2SO_4, and 10 mL of $H_3(PO_4)_3$ were mixed in a round-bottom flask. The mixture was then heated in an oil bath and kept at 55 °C for 12 h. After that, the mixture was poured onto a DI water ice bath, and then 30% H_2O_2 was added until the color changed from purple to dark yellow. The mixture was then centrifuged, the supernatant poured off, and then the pellet was washed with 37% HCl/water/ethanol (volume ratio 1:1:1) twice and ethanol once. The left-over powder was placed into a vacuum oven at room temperature and dried overnight. For the steps of the Ni and N doping process, it follows the same procedure as described above for cornstarch-based catalysts, but using 1.0 g of graphene oxide in place of 1.0 g of cornstarch, and only using a 500 ppm Ni solution as the Ni feedstock. This sample was named GO-N-Ni-500.

2.1.3 Synthesis of CS-N-Ni via wet impregnation

Another comparison sample was prepared using cornstarch as the carbon feedstock, but a widely used wet impregnation method to dope Ni in carbon, noted as CS-N-Ni-WI. It was designed to have the same weight percent of Ni as that in CS-N-Ni-500, which was pre-determined by ICP-MS analysis of the Ni content. To synthesize CS-N-Ni-WI, 100 mg of cornstarch and 1.0 g of urea were dispersed into 20 mL of water, and the mixture was stirred, open to the atmosphere under heating maintained at 50 °C. After the solids were well dispersed, 100 µg of Ni as in $Ni(NO_3)_2$, equivalent to the same wt% of Ni in pre-pyrolysis CS-N-Ni-500, was added dropwise into the solution. The solution was left until fully evaporated, after which it was collected and ground to a fine powder. Pyrolysis was carried out the same as described above for CS-N-Ni-X samples.

2.2 Materials Characterization

Scanning electron microscopy (SEM, JEOL JSM7500F) was used to study the morphology of prepared catalysts. X-ray photoelectron spectroscopy (XPS, Omicron) was used to characterize the surface elemental composition of N species. Inductively coupled plasma mass spectrometry (ICP-MS, Agilent 7700x icp-ms) was used to measure the atomic metal contents in the catalysts. Proton nuclear magnetic resonance (1H NMR, Bruker 400 MHz spectrometer) was used to identify liquid products, if any, produced in electrochemical CO_2RR.

2.3 Electrochemical CO_2RR Activity Measurements

The electrochemical CO_2RR activity measurements were conducted in a two-compartment H-cell in CO_2-saturated $KHCO_3$ electrolyte (0.5 M) with a three-electrode system. Platinum foil (1 cm^2) was used as the counter electrode for oxygen evolution reaction in the anode compartment and an Ag/AgCl (3M KCl) electrode was used as the reference electrode in the cathode compartment. All electrochemical tests were conducted with a Gamry Reference 3000 electrochemical working station (Gamry Instruments). The measured potentials after *iR*-compensation were rescaled to the reversible hydrogen electrode (RHE) by E(RHE) = E(Ag/AgCl) + 0.210V + 0.0591V × pH, where the pH was 7.2 for a solution of 0.5M $KHCO_3$ saturated by CO_2. The working electrode was prepared by drop casting catalyst ink onto carbon paper (Toray, TGP-H-060). The ink was prepared by dispersing 3 mg catalysts into a mixture of 370 µL of ethanol, 200 µL of DI-water, and 30 µL of 5% Nafion solution

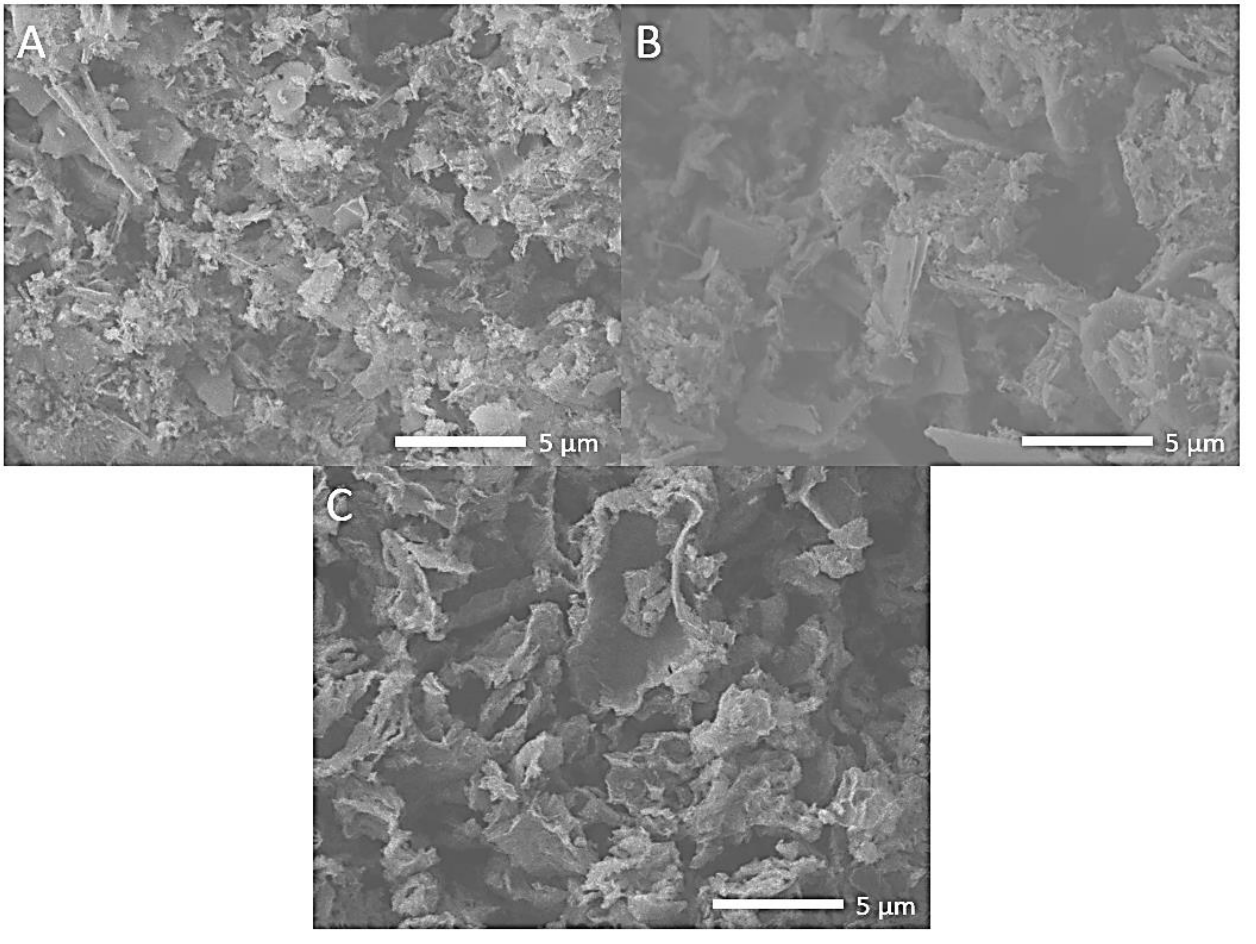

Fig. 2 SEM images of (A) CS, (B) CS-N-Ni, and (C) GO-N-Ni.

(Chemours, D520) which was then sonicated for 2 h. After the 2 h, the ink was cast with a catalytic geometric area of 1 cm^2 and a catalyst mass loading of 1.0 mg/cm^2. After drying, the working electrode was placed into the cathode chamber with the reference electrode. The anode and cathode compartments were separated by a Nafion 115 (Chemours) proton exchange membrane which served to avoid re-oxidation of CO_2RR generated products. High purity CO_2 (Airgas, 99.999%), with a flow rate of 38 mL/min, which was maintained during the whole process was first introduced into the cathode chamber for 30 min before electrolysis to fully saturate the electrolyte. The gas-phase products from the H-Cell cathode compartment were analyzed by an online gas chromatograph (GC, Fuel Cell GC-2014ATF, Shimadzu), which was equipped with a thermal conductivity detector (TCD) and a methanizer assisted flame ionization detector (FID).

3. Results and Discussion

3.1 Structure and Composition Characterizations

Fig. 2 shows the morphology of CS, CS-N-Ni, and GO-N-Ni characterized by SEM, which reveals that the cornstarch-based catalyst contains disordered layered structures intermixed with fine flakes, while the doping of N and Ni does not significantly affect its morphology. The GO based catalyst has a more delaminated layer structure intermixed with fine flakes. The Nyquist plots by electrochemical impedance spectroscopy (EIS) were obtained and compiled in Fig. 3A for samples CS-N, CS-N-Ni-500, GO-N-Ni-500, and CS-N-Ni-WI, and the equivalent circuit model of the cathode side compartment for the H-cell was defined in Fig. 3B. In the equivalent circuit model, the solution resistance (R_S) was assigned to the intercept on the real axis. The first semicircle which was assigned as the Ohmic resistance (R_Ω), represents the conductivity of the catalysts. The last resistance was assigned as the charge transfer resistance (R_{CT}), which represents the resistance the electrons underwent transferring from the catalyst to the reactants. The elements Q1 and Q2 represent the constant phase elements which are in parallel with R_Ω and R_{CT} respectively, corresponding to the capacitance together with each resistance.[29,30] The fitting results can be found in Table S1. Solution and ohmic resistance were similar for all groups (R_S = 1.4-1.8 Ω) (R_Ω = 1.7−2.7 Ω). However, the metal-free, CS-N, group showed a larger charge-transfer resistance (R_{CT} = 250 Ω) than the other metal containing samples, suggesting that the presence of Metal−N active sites accelerates the transfer of electrons, which is supported by the increase in catalytic active reported below. All the metal containing samples showed a similar charge-transfer resistance (R_{CT} = ~20 Ω). The electrochemical surface area (ECSA) via double-layer capacitance (C_{dl}), was

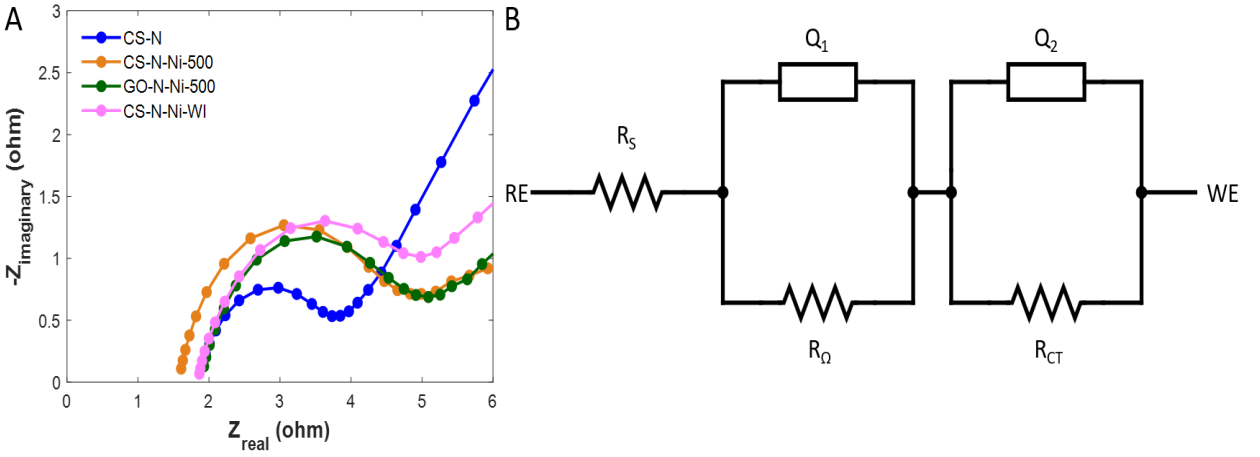

Fig. 3 (A) Nyquist plots at -0.8 V versus. RHE and (B) the equivalent circuit of the H-cell cathode side compartment, where R_S is the solution resistance, R_Ω the ohmic resistance, and R_{CT} the charge transfer resistance. Q1 and Q2 represent the constant phase elements.[29]

measured using cyclic voltammograms, as seen in Fig. S2 and S3. GO-N-Ni-500 showed the largest C_{dl} (29.2 mF/cm^2) followed by CS-N-Ni-500 (14.3 mF/cm^2) and CS-N-Ni-WI (13.8 mF/cm^2). This difference in C_{dl} shows that the GO based catalyst has a higher C_{dl} or ECSA than the cornstarch based one, but as discussed later in the paper, not necessarily an increased catalytic performance in terms of product selectivity.

To compare Ni adsorption capabilities as well as to aid in the comparison of differences found from electrochemical performance, ICP-MS data were collected for CS-N-Ni-500 and GO-N-Ni-500 before and after pyrolysis, as shown in Table S2. GO was able to adsorb more nickel than cornstarch was with pre-pyrolysis GO-N-Ni-500 having a Ni wt% 10 times greater than that of pre-pyrolysis CS-N-Ni-500. This is most likely due to the large density of well exposed oxygen functional groups found on GO.[31] As can been seen from Fig. S1, while cornstarch has a large density of oxygen functional groups, many of them are in such close proximity to one another that they will interfere with the adsorption of Ni, while others are found in the middle of the structure, lowering its ability to adsorb Ni. The Ni wt% found in CS-N-Ni-500 and GO-N-Ni-500 both increase due to the loss of carbon, oxygen, and hydrogen elements during pyrolysis, while GO-N-Ni-500 maintains a Ni content (2.8 wt%) 10 times larger than CS-N-Ni-500 (0.26 wt%).

The surface elemental composition of N species was determined by X-ray photoelectron spectroscopy (XPS). It was determined by XPS that N 1s was located at 400 eV, the full range of XPS can be found in Fig. S4. The N concentrations were found to be 7 and 8 wt % for CS-N and CS-N-Ni-500 respectively. The similarity in N content between metal-free and metal containing groups, is most likely due to N-doping being mostly determined by carbon and N sources, as well as the pyrolysis temperature, thus not being affected by the presence of Ni.[32] High-resolution XPS spectra of N 1S was further used to determine the configuration of N dopants. For each sample, results found in Fig. 4, CS, CS-N, and CS-N-Ni-500, the N 1S curve was fitted by four curves. The curves represented pyridinic N centered at around 398.2 eV, pyrrolic N centered at around 400.5 eV, graphitic N centered at around 401.3 eV, and oxidized like N centered at around 403 eV.[33-35] Previous reports have demonstrated that the electronic environment of N atoms found in M–N–C sites can be altered as compared to just C-N sites.[36,37] This change is verified when comparing the N 1s spectra of metal containing and metal free groups, which is a commonly used to verify the formation of M-N sites.[38,39] It can be seen from Fig. 4A that the pyridinic-N position for CS-N is centered at 398.3 eV while there is a positive shift to 398.5 eV for CS-N-Ni-500. The other N species, pyrrolic, graphitic, and oxidized like, show no noticeable shift between metal containing and metal-free groups. This shift of pyridinic N is consistent with previous reports that state the binding energy of pyridinic N shifts to a higher value when a chemical bond is formed between metal and N atoms.[33,40,41]

3.2 Electrochemical CO_2 Reduction Reaction Performance

Linear sweep voltammetry (LSV) was first tested, as seen in Fig. 5A, under an Ar saturated condition and a CO_2 saturated condition, with a potential range of -0.2 V to -1.0 V versus RHE. The current of CS-N-Ni-500 had a greater (absolute) slope, after -0.5 V, under CO_2 saturation than under Ar saturation. The activity under Ar saturation can be contributed to HER, while the increase in activity under CO_2 saturation can be attributed to the presence of the electrochemical CO_2RR.

Next, electrochemical CO_2RR was carried out in the range of -0.5 V to -1.0 V versus RHE for CS, CS-N, and CS-N-Ni-X catalysts prepared with different Ni concentration solutions (10 – 1000 ppm). CO and H_2 were detected as the main products for the entire potential range, while only a trace amount of CH_4 (less than 1 ppm or 0.2% faradaic efficiency (FE) for CH_4) was detected at potentials -0.9 and -1.0 V versus RHE, as shown in Table S3. Fig. S5 shows that no liquid

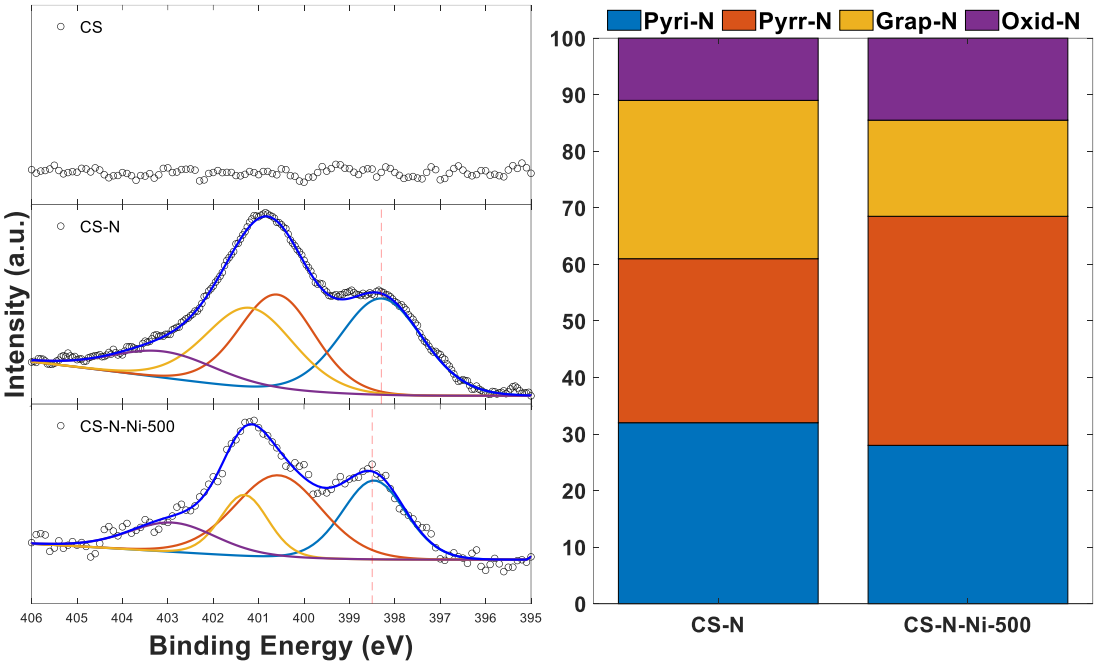

Fig. 4 (A) High-resolution XPS spectra of the N 1S peaks found in CS, CS-N, and CS-N-Ni-500 and (B) the distribution of N species found in CS-N and CS-N-Ni-500.

products such as HCOOH could be detected by 1 H NMR after a two-hour run at -0.8 V versus RHE. Figs. 5B-5D present the total current density, FE(CO), and CO current density, respectively, for CS, CS-N, and CS-N-Ni-X catalysts at the potential range of -0.5 V to -1.0 V versus RHE. The carbon only group CS had minimal performance never achieving an FE (CO) greater than 1%; the current generated was mainly attributed to hydrogen evolution. The Ni free group CS-N showed its highest CO selectivity of 50% and a total current density of less than 0.2 mA/cm^2 at -0.5 V versus RHE. Compared with the metal free group, all Ni-doped groups, regardless of Ni concentration during synthesis, achieved

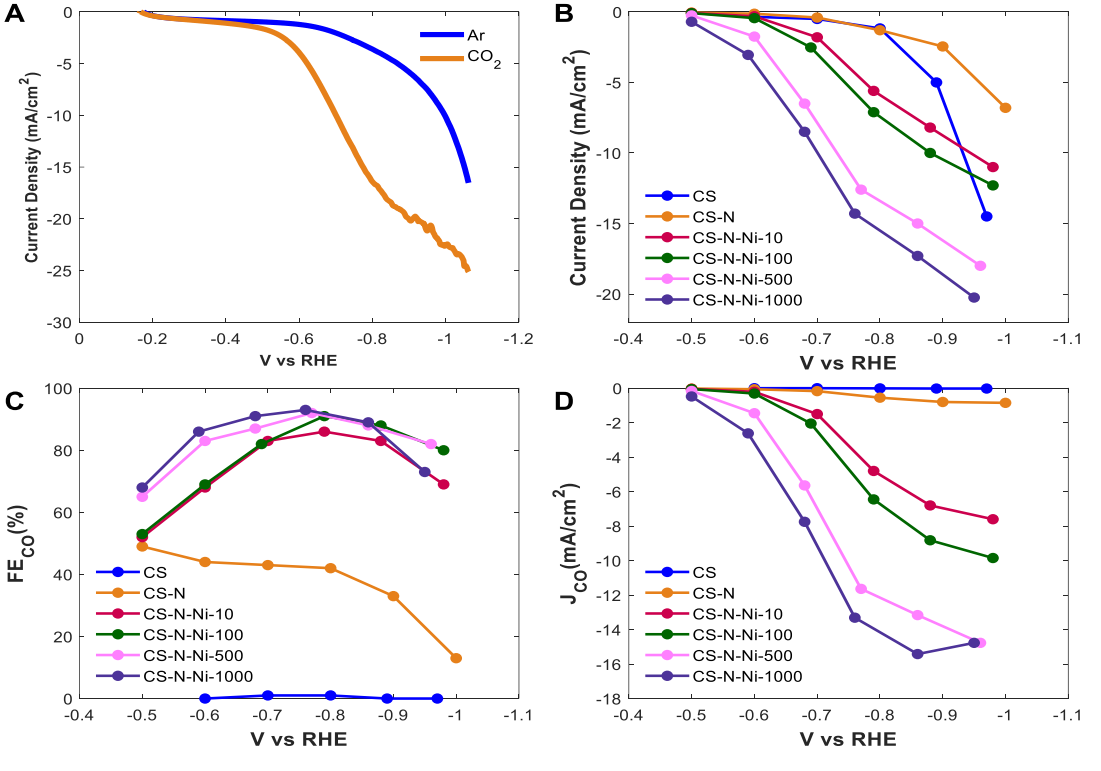

Fig. 5 (A) LSV curves recorded on CS-N-Ni-500 under Ar and CO_2 saturated conditions at a scan rate of 5 mV·s^{-1}, (B) total current density, (C) Faradaic efficiency of CO production, and (D) CO current density of CS, CS-N, and CS-N-Ni-X catalysts (X = 10 – 1000).

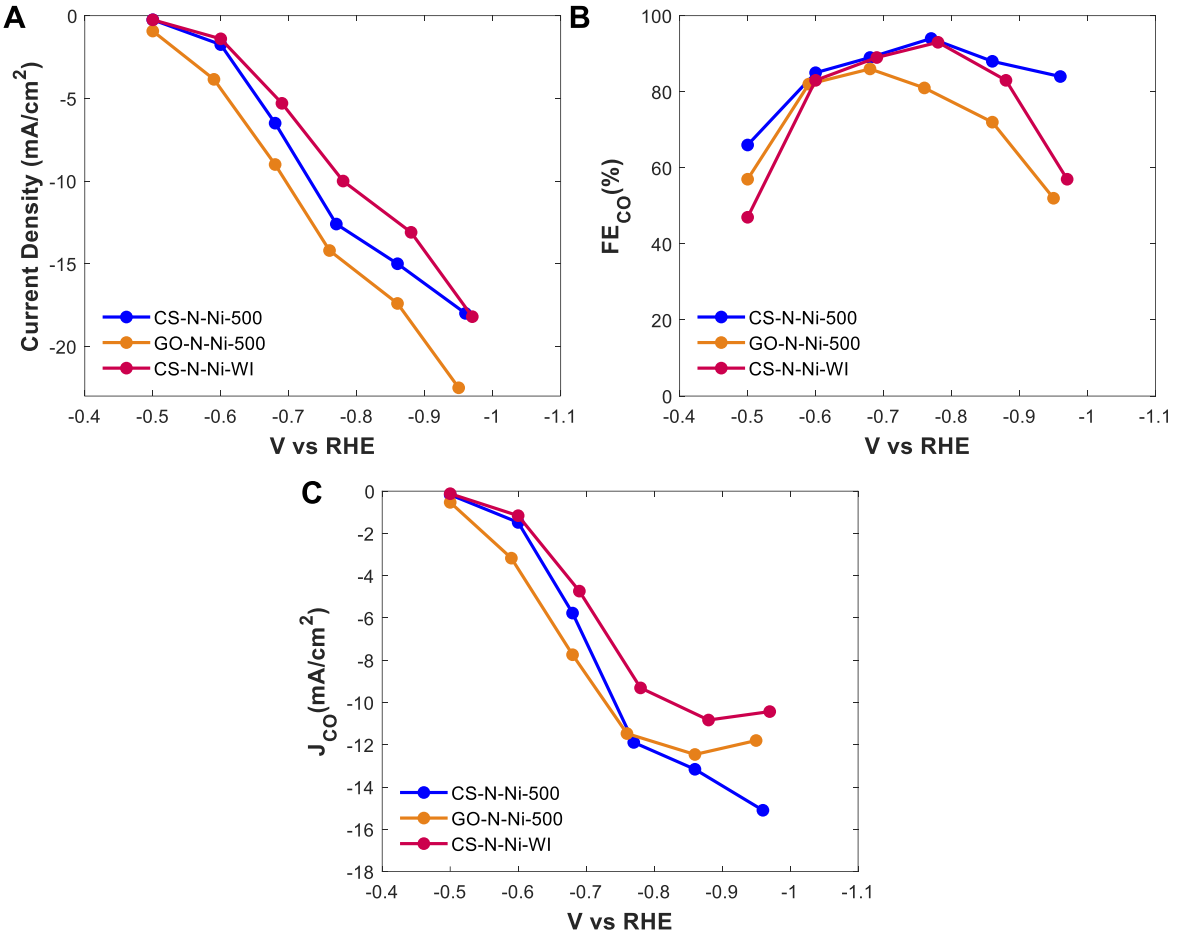

Fig. 6 (A) Total current density, (B) Faradaic efficiency of CO production, and (C) CO current density of CS-N-Ni-500, GO-N-Ni-500, and CS-N-Ni-W.

a better CO selectivity and larger current density. This result confirms that N and Ni doping provided active sites for CO_2RR. The FE (CO) peaked at -0.8 V versus RHE for all CS-N-Ni-X catalysts. The overall FE (CO) increased with Ni concentration used from 10 to 500 ppm but stagnated after 500 ppm. Accordingly, the two metal free groups (CS and CS-N) had the highest FE (H_2), while all metal containing groups (CS-N-Ni-X) showed the same low selectivity for H_2 production, as seen in Fig. S6. The best combination of FE (CO), CO current density, potential range of max performance, were CS-N-Ni-500 with a CO current density of 11.6 mA/cm^2 and a FE (CO) of 92% at -0.8 V versus RHE and CS-N-Ni-1000 with a CO current density of 13.3 mA and a 93% FE (CO) at the same potential. These results demonstrate that using a solution with a Ni concentration in the range of 500 – 1000 ppm produces the best performance, but also show that if the source of the Ni solution has a smaller concentration, a catalyst can still be produced with a satisfactory FE(CO).

The stability of CS-N-Ni-500 was tested for 24 h at -0.8 V versus RHE where the FE (CO) reached its maximum, and the results are shown in Fig. S7. The current density dropped off quickly during the first five hours of operation, but then showed only a gradual decrease from five hours until the end of the test. While the current density varied with time, the FE (CO) remained mostly constant around 90% throughout the duration of the test. The results indicate that the stability of FE (CO) was excellent but that of the current density has room to improve, which could be the topic of our next work.

We believe the majority of Ni metal exist in the single atomic phase and the active sites are Ni-N-C. To support the claim, we have done two experiments. First, the electrochemical performance of CS-N-Ni-500 was compared to that of CS-N-Ni-500-AW, the acid-washed version of catalyst likely having only atomic sites. As shown in Fig. S8, both catalysts had a similar total current density with CS-N-Ni-500-AW showing only a slight decrease in CO selectivity, indicating similar materials structure of the two samples. Second, we tested the magnetic properties of the catalysts using a strong neodymium magnet. While GO-N-Ni-500 and CS-N-Ni-WI showed magnetic properties, CS-N-Ni-500 did not. It has been reported that Ni nanoparticles are ferromagnetic,[42] but single atomic Ni adsorbed onto graphdiyne and graphyne showed no magnetic moment.[43] Thus, we believe the above two experiments provided indirect evidence that the status of Ni is single atomic in the CS-N-Ni-500 and likely other CS-N-Ni-X catalysts and that post-treatment acid wash is not necessary to achieve the single atomic status when using this novel synthesis method.

3.3 Comparison of CO_2RR activity with benchmark catalysts

The CO_2RR performance of the cornstarch-based, Ni-adsorption method synthesized catalyst (CS-N-Ni-500) was compared with those of two benchmark catalysts: (1) GO-N-Ni-500, which was synthesized by the same method except using GO as the carbon source, and (2) CS-N-Ni-WI, which was synthesized using cornstarch but a different method, wet impregnation, to dope Ni and N at the same Ni content level. The comparison data regarding total current density, FE(CO), and CO current density are shown in Fig. 6. By examining the entire applied potential range, for total current density, it follows the order of GO-N-Ni-500 > CS-N-Ni-500 > CS-N-Ni-WI; however, for FE(CO), it follows the order of CS-N-Ni-500 > CS-N-Ni-WI > GO-N-Ni-500. In other words, GO-N-Ni-500 has the highest total current density but lowest selectivity for CO production (or highest selectivity for H_2 production). The highest total current density is reasonable given that (1) GO-N-Ni-500 has the highest C_{dl} or ECSA (Fig. S3), twice as much as that of CS-N-Ni-500, and (2) GO-N-Ni-500 has a much higher Ni content (2.8 wt%) than that of CS-N-Ni-500 (0.26 wt%), and as a result, a larger number of active sites of Ni-N. On the other hand, this high Ni content in GO-N-Ni-500 may tend to form aggregates of Ni nanoparticles as opposed to dispersed Ni-N sites, thus favoring HER over CO_2RR.[13] This can possibly explain the lower CO selectivity and the higher H_2 selectivity by GO-N-Ni-500 than by CS-N-Ni-500, as shown in Fig. S9. This result again confirms that it is not necessarily preferred to have a high Ni content in CO_2RR catalysts, which is the possible reason post acid wash has been widely applied to remove the metal nanoparticles and leave only dispersed M-N sites. When compared with the wet impregnation prepared sample, CS-N-Ni-WI, the adsorption method prepared sample CS-N-Ni-500 also demonstrates a higher CO selectivity, a lower H_2 selectivity, and a higher current density, although both samples are based on cornstarch and have the same level of Ni content. The result suggests that Ni adsorption onto cornstarch via ion-dipole adsorption on surface oxygen functional groups is a preferred way of synthesizing dispersed active M-N-C sites than a conventional wet impregnation method.

Furthermore, when comparing the performance of the catalysts developed in this work with the state-of-the-art catalysts reported in the literature, as seen in Table S4, our catalysts compared equally, if not better, under the same testing conditions, but we used an abundant biomaterial-based carbon source, and avoided acid/ethanol washing, while others used more expensive carbon precursors or preformed acid/ethanol washes. Because of the ease of synthesis, the use of cheaper and sustainable feedstock, and the excellent catalytic performance, the cornstarch-based, Ni-adsorption method synthesized catalysts developed in this work could potentially pave a way to the application of large-scale CO_2 utilization in a cost-effective and sustainable manner.

4. Conclusions

In summary, we demonstrated the synthesis of an efficient M-N-C catalyst for CO_2RR using a cheap, abundant biomaterial feedstock, as well as a sustainable method that does not create harmful wastes, but rather, could potentially utilize industrial waste streams that contain heavy metals such as Ni. Examples of such synthesized catalysts, CS-N-Ni-500 and CS-N-Ni-1000, by adsorbing Ni from 500 and 1000 ppm Ni solutions, respectively, showed excellent CO_2RR activities. CS-N-Ni-500 achieved a 92% FE (CO) with a CO current density of 11.6 mA/cm^2, while CS-N-Ni-1000 achieved a 93% FE (CO) with a CO current density of 13.3 mA/cm^2 at −0.8 V versus RHE. The effectiveness of the cornstarch-based catalyst CS-N-Ni-500 was evaluated by comparing its catalytic performance with a widely used graphene oxide-base catalyst, GO-N-Ni-500, synthesized by the same method. Although GO-N-Ni-500 resulted in a higher total current because of its higher Ni content, it underperformed CS-N-Ni-500 in terms of FE (CO) and CO current density, likely due to the formation of Ni aggregates on GO-N-Ni-500 that favor HER over CO_2RR. The advantage of this synthesis method was further verified by comparing CS-N-Ni-500 against a catalyst prepared by a conventional wet impregnation method, CS-N-Ni-WI, with the same Ni content in the catalyst. Again, CS-N-Ni-500 outperformed CS-N-Ni-WI in terms of both CO selectivity and current density. The cornstarch-based, Ni-adsorption synthesized catalysts developed in this work also show comparable performance to those in the literature using more expensive materials and less environmentally friendly methods. Findings in this work suggest the potential for large-scale manufacturing of cost-effective CO_2RR catalysts using cheap, abundant biomaterials and waste sources as the feedstock while avoiding the generation of wastes from the synthesis process, thus enhancing the overall sustainability of the CO_2RR technology. The unique structure of the catalyst reported in this work could also be applied in other catalytic applications such as oxygen reduction or CO reduction reactions that could be explored as a future topic.

Acknowledgements

This work was supported by the U.S. National Science Foundation (NSF CBET #1805132). The use of the Texas A&M University Materials Characterization Facility is also acknowledged.

Supporting Information

Additional SEM images, additional electrocatalytic performance for various comparison catalyst, product concentration detected by GC, ^{1}H NMR analysis for liquid product, XPS survey spectra, CV curves analyzing ESCA, performance comparison against previous reports, and catalyst concentration measured by ICP–MS.

Conflict of Interest

There is no conflict of interest.

References

[1] U.S.A. EPA, *Food: Material-Specific Data* (2017 https://www.epa.gov/facts-and-figures-about-materials-waste-and-recycling/food-material-specific-data).

[2] U.S.A. EPA, *Inventory of U.S. Greenhouse Gas Emissions and Sinks* (2017 https://www.epa.gov/ghgemissions/inventory-us-greenhouse-gas-emissions-and-sinks).

[3] O. B. Akpor, G. O. Ohiobor, T. D. Olaolu, *Adv. Biosci. Bioeng.,* 2014, **2**, 37, doi: 10.11648/j.abb.20140204.11.

[4] M. A. Barakat, *Arab. J. Chem.,* 2011, **4**, 361-377, doi: 10.1016/j.arabjc.2010.07.019.

[5] E. Epstein, The Science of Composting, CRC Press, 2017, pp. 504, doi: 10.1201/9780203736005.

[6] P. K. Pandey, S. Choubey, Y. Verma, M. Pandey, S. S. Kalyan Kamal, K. Chandrashekhar, *Int. J. Environ. Res. Public Health,* 2007, **4**, 332-339, doi: 10.3390/ijerph200704040009.

[7] M. G. Kibria, J. P. Edwards, C. M. Gabardo, C. T. Dinh, A. Seifitokaldani, D. Sinton, E. H. Sargent, *Adv. Mater.,* 2019, **31**, 1807166, doi: 10.1002/adma.201807166.

[8] Y. Gang, F. Pan, Y. Fei, Z. Du, Y. H. Hu, Y. Li, *ACS Sustain. Chem. Eng.,* 2020, **8**, 8840-8847, doi: 10.1021/acssuschemeng.0c03054.

[9] X. Hao, X. An, A. M. Patil, P. Wang, X. Ma, X. Du, X. Hao, A. Abudula, G. Guan, *ACS Appl. Mater. Interfaces,* 2021, **13**, 3738-3747, doi: 10.1021/acsami.0c13440.

[10] N. Wang, Z. Liu, J. Ma, J. Liu, P. Zhou, Y. Chao, C. Ma, X. Bo, J. Liu, Y. Hei, Y. Bi, M. Sun, M. Cao, H. Zhang, F. Chang, H.-L. Wang, P. Xu, Z. Hu, J. Bai, H. Sun, G. Hu, M. Zhou, *ACS Sustain. Chem. Eng,* 2020, **8**, 13813-13822, doi: 10.1021/acssuschemeng.0c05158.

[11] F. Pan, B. Li, E. Sarnello, Y. Fei, X. Feng, Y. Gang, X. Xiang, L. Fang, T. Li, Y. H. Hu, G. Wang, Y. Li, *ACS Catal.,* 2020, **10**, 10803-10811, doi: 10.1021/acscatal.0c02499.

[12] C. Zhang, S. Yang, J. Wu, M. Liu, S. Yazdi, M. Ren, J. Sha, J. Zhong, K. Nie, A. S. Jalilov, Z. Li, H. Li, B. I. Yakobson, Q. Wu, E. Ringe, H. Xu, P. M. Ajayan, J. M. Tour, *Adv. Energy Mater.,* 2018, **8**, 1703487, doi: 10.1002/aenm.201703487.

[13] K. Jiang, S. Siahrostami, T. Zheng, Y. Hu, S. Hwang, E. Stavitski, Y. Peng, J. Dynes, M. Gangisetty, D. Su, K. Attenkofer, H. Wang, *Energy Environ. Sci.,* 2018, **11**, 893-903, doi: 10.1039/C7EE03245E.

[14] Z. Wang, P. Hou, Y. Wang, X. Xiang, P. Kang, *ACS Sustain. Chem. Eng,* 2019, **7**, 6106-6112, doi: 10.1021/acssuschemeng.8b06278.

[15] T. Möller, W. Ju, A. Bagger, X. Wang, F. Luo, T. N. Thanh, A. S. Varela, J. Rossmeisl, P. Strasser, *Energy Environ. Sci.,* 2019, **12**, 640-647, doi: 10.1039/C8EE02662A.

[16] Q. Fan, P. Hou, C. Choi, T.-S. Wu, S. Hong, F. Li, Y.-L. Soo, P. Kang, Y. Jung, Z. Sun, *Adv. Energy Mater.,* 2020, **10**, 1903068, doi: 10.1002/aenm.201903068.

[17] S. Ghosh, S. Ramaprabhu, *J. Colloid Interf. Sci.,* 2020, **559**, 169-177, doi: 10.1016/j.jcis.2019.10.030.

[18] F. Pan, H. Zhao, W. Deng, X. Feng, Y. Li, *Electrochim. Acta,* 2018, **273**, 154-161, doi: 10.1016/j.electacta.2018.04.047.

[19] F. Pan, H. Zhang, Z. Liu, D. Cullen, K. Liu, K. More, G. Wu, G. Wang, Y. Li, *J. Mater. Chem. A,* 2019, **7**, 26231-26237, doi: 10.1039/C9TA08862H.

[20] T. N. Huan, N. Ranjbar, G. Rousse, M. Sougrati, A. Zitolo, V. Mougel, F. Jaouen, M. Fontecave, *ACS Catal.,* 2017, **7**, 1520-1525, doi: 10.1021/acscatal.6b03353.

[21] C. Zhao, X. Dai, T. Yao, W. Chen, X. Wang, J. Wang, J. Yang, S. Wei, Y. Wu, Y. Li, *J. Am. Chem. Soc.,* 2017, **139**, 8078-8081, doi: 10.1021/jacs.7b02736.

[22] Q. He, D. Liu, J. H. Lee, Y. Liu, Z. Xie, S. Hwang, S. Kattel, L. Song, J. G. Chen, *Angew. Chem. Int. Ed.,* 2020, **59**, 3033-3037, doi: 10.1002/anie.201912719.

[23] "Corn Starch Market Size, Share and Industry Analysis By Type (Native Starch, Modified Starch, and Sweeteners), Application (Food and Beverage, Animal Feed, Paper and Board, and Others), and Regional Forecast 2019 - 2026," *FBI. Mkt. Res. Rep.* (2019).

[24] J. O. Duruibe, M. O. C. Ogwuegbu, J. N. Egwurugwu, *Int. J. Phys. Sci.,* 2007, **2**, 112-118, doi: 10.5897/IJPS.

[25] U. Okereafor, M. Makhatha, L. Mekuto, N. Uche-Okereafor, T. Sebola, V. Mavumengwana, *Int. J. Environ. Res. Public Health*, 2020,7, 2204, doi: 10.3390/ijerph17072204

[26] P. Meshram, A. Dhar Pandey, B. Dhar Pandey, *Miner. Process. Extr. Metall. Rev.*, 2019, **3**, 157-193, doi: 10.1080/08827508.2018.1514300

[27] V. Agarwal, M. K. Khalid, A. Porvali, B. P. Wilson, M. Lundström, *Sustain. Mater. Techno.,* 2019, **22**, e00121, doi: 10.1016/j.susmat.2019.e00121.

[28] D. C. Marcano, D. V. Kosynkin, J. M. Berlin, A. Sinitskii, Z. Sun, A. Slesarev, L. B. Alemany, W. Lu, J. M. Tour, *ACS Nano,* 2010, **4**, 4806-4814, doi: 10.1021/nn1006368.

[29] D. H. Won, H. Shin, J. Koh, J. Chung, H. S. Lee, H. Kim, S. I. Woo, *Angew. Chem. Int. Ed.,* 2016, **55**, 9297-9300, doi: 10.1002/anie.201602888.

[30] F. Pan, B. Li, W. Deng, Z. Du, Y. Gang, G. Wang, Y. Li, *Appl. Catal. B.,* 2019, **252**, 240-249, doi: 10.1016/j.apcatb.2019.04.025.

[31] K. Erickson, R. Erni, Z. Lee, N. Alem, W. Gannett, A. Zettl, *Adv. Mater.,* 2010, **22**, 4467-4472, doi: 10.1002/adma.201000732.

[32] Z.-H. Sheng, L. Shao, J.-J. Chen, W.-J. Bao, F.-B. Wang, X.-H. Xia, *ACS Nano,* 2011, **5**, 4350-4358, doi: 10.1021/nn103584t.

[33] F. Pan, W. Deng, C. Justiniano, Y. Li, *Appl. Catal. B.,* 2018, **226**, 463-472, doi: doi: 10.1016/j.apcatb.2018.01.001.

[34] T. Zheng, K. Jiang, N. Ta, Y. Hu, J. Zeng, J. Liu, H. Wang, *Joule,* 2019, **3**, 265-278, doi: 10.1016/j.joule.2018.10.015.

[35] H. Wang, F.-X. Yin, N. Liu, R.-H. Kou, X.-B. He, C.-J. Sun, B.-H. Chen, D.-J. Liu, H.-Q. Yin, *Adv. Funct. Mater.,* 2019, **29**, 1901531, doi: 10.1002/adfm.201901531.

[36] G. Wu, C. M. Johnston, N. H. Mack, K. Artyushkova, M. Ferrandon, M. Nelson, J. S. Lezama-Pacheco, S. D. Conradson, K. L. More, D. J. Myers, P. Zelenay, *J. Mater. Chem.,* 2011, **21**, 11392-11405, doi: 10.1039/C0JM03613G.

[37] H.-W. Liang, W. Wei, Z.-S. Wu, X. Feng, K. Müllen, *J. Am. Chem. Soc.,* 2013, **135**, 16002-16005, doi: 10.1021/ja407552k.

[38] M. Salavati-Niasari, A. Amiri, *Appl. Catal. A-GEN.,* 2005, **290**, 46-53, doi: 10.1016/j.apcata.2005.05.009.

[39] X. Cui, S. Yang, X. Yan, J. Leng, S. Shuang, P. M. Ajayan, Z. Zhang, *Adv. Funct. Mater.,* 2016, **26**, 5708-5717, doi: 10.1002/adfm.201601492.
[40] X. Li, W. Bi, M. Chen, Y. Sun, H. Ju, W. Yan, J. Zhu, X. Wu, W. Chu, C. Wu, Y. Xie, *J. Am. Chem. Soc.,* 2017, **139**, 14889-14892, doi: 10.1021/jacs.7b09074.
[41] H. Fei, J. Dong, M. J. Arellano-Jiménez, G. Ye, N. Dong Kim, E. L. G. Samuel, Z. Peng, Z. Zhu, F. Qin, J. Bao, M. J. Yacaman, P. M. Ajayan, D. Chen, J. M. Tour, *Nat. Commun.,* 2015, **6**, 8668, doi: 10.1038/ncomms9668.
[42] X. He, H. Shi, *Particuology,* 2012, **10**, 497-502, doi: 10.1016/j.partic.2011.11.011.
[43] J. He, S. Y. Ma, P. Zhou, C. X. Zhang, C. He, L. Z. Sun, *J. Phys. Chem. C,* 2012, **116**, 26313-26321, doi: 10.1021/jp307408u.

Author information

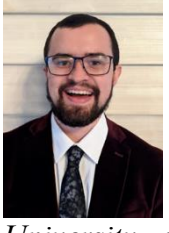

John Edward Pellessier *is a Ph.D. student in the J. Mike Walker 66' Department of Mechanical Engineering at Texas A&M University. He received his B.S. degree in both Mechanical Engineering and Chemistry from the University of Portland. He is interested in the sustainable synthesis of electrofuels through electrochemical reduction of* CO_2 *and water splitting to promote sustainable energy.*

Yang Gang *received his B.S. degree in Shanghai Jiao Tong University and M.S. degree in The Hong Kong University of Science and Technology both in Mechanical Engineering. He is currently pursuing Ph.D. degree in the J. Mike Walker 66' Department of Mechanical Engineering at Texas A&M University. His research interest is electrochemical* CO_2 *reduction.*

Ying Li *is a Professor and Pioneer Natural Resources Faculty Fellow in the J. Mike Walker '66 Department of Mechanical Engineering at Texas A&M University. He received his Ph.D. degree in Environmental Engineering Sciences from University of Florida in 2007. His current research focuses on nanomaterials and catalysis for clean energy and environmental sustainability, including solar energy harvesting and conversion, carbon capture and utilization, rechargeable batteries, water treatment and desalination, and air pollution control. He has published 90 refereed journal articles. He received the National Science Foundation (NSF) CAREER Award in 2013.*